# Position Tracking for a Nonlinear Underactuated Hovercraft: Controller Design and Experimental Results

António Pedro Aguiar
Department of Electrical and Computer Engineering
University of California
Santa Barbara, CA 93106, USA
aguiar@ece.ucsb.edu

Lars Cremean
Department of Mechanical Engineering
California Institute of Technology
Pasadena, CA 91125, USA
lars@caltech.edu

João Pedro Hespanha
Department of Electrical and Computer Engineering
University of California
Santa Barbara, CA 93106, USA
hespanha@ece.ucsb.edu

***Abstract*— This paper addresses the position tracking control problem of an underactuated hovercraft vehicle. A nonlinear Lyapunov-based tracking controller is developed and proved to exponentially stabilize the position tracking error to a neighborhood of the origin that can be made arbitrarily small. The desired trajectory does not need to be a specially chosen (*e.g.*, a trimming trajectory). In fact, it can be any sufficiently smooth bounded curve parameterized by time. The nonlinear controller has been experimentally validated on the Caltech Multi-Vehicle Wireless Testbed (MVWT), a platform for the development and implementation of novel single- and multiple-vehicle control designs. Experimental results are given for tracking of prescribed trajectories and for target following.**

## I. Introduction

The past few decades have witnessed an increased research effort in the area of trajectory tracking control for underactuated autonomous vehicles. Trajectory tracking problems are concerned with the design of control laws that force a vehicle to reach and follow a time parameterized reference (*i.e.*, a geometric path with an associated timing law). The degree of difficulty involved in solving these problems is highly dependent on the configuration of the vehicle. For fully actuated systems, the trajectory tracking problem is now reasonably well understood [13, 17, 21].

For underactuated autonomous vehicles, *i.e.*, systems with a smaller number of control inputs than the number of independent generalized coordinates [23], trajectory tracking is still an active research topic. The study of these systems is motivated by the fact that it is usually costly and often impractical (due to weight, reliability, complexity, and efficiency considerations) to fully actuate autonomous vehicles. Typical examples of underactuated systems include robot manipulators, wheeled robots, walking robots, spacecraft, aircraft, helicopters, missiles, surface vessels, and underwater vehicles. The tracking problem for underactuated vehicles is especially challenging because most of these systems are not fully feedback linearizable and exhibit nonholonomic constraints, therefore standard tools used to control nonlinear systems—such as feedback linearization and integrator backstepping—are not directly applicable. See [20] for a survey of these concepts and [6] for a framework to study the controllability and the design of motion algorithms for underactuated Lagrangian systems on Lie groups.

A class of underactuated vehicles that poses considerable challenging in control system design is the class of marine underactuated vehicles. These vehicles exhibit complex hydrodynamic effects that must necessarily be taken into account during the control design. This is in striking contrast with mobile wheeled robots, where methodologies that build on pure vehicle kinematics are often adequate for control. It is relevant to point out that many marine vehicle models exhibit a drift vector field that is not in the span of the input vector fields, thus precluding the use of input transformations to bring them to driftless form.

Fig. 1. The MVWT vehicle. A laptop is secured in a Plexiglas chassis that glides on omnidirectional ball casters. Software-controlled high-powered ducted fans attached to the vehicle provide thrust. A MVWT signature on the top the vehicle ( a "hat") is identified by overhead cameras, and the vehicle receives its position and orientation in a GPS-like fashion over a local wireless network.

Hovercrafts are another type of vehicles with a structure model similar to marine vehicles. A model for an underactuated hovercraft was obtained in [9] from the equations of a simplified ship and several control strategies are described for positioning the vehicle.

The classical approach for trajectory tracking of underactuated marine vehicles utilizes local linearization and coordinates decoupling to steer the same number of degrees of freedom as the number of available control inputs. This can be done using standard linear (or nonlinear) control methods [10]. Alternative approaches include the linearization of the vehicle error dynamics about trajectories that lead to a time-invariant linear system (also known as trimming trajectories) combined with gain scheduling and/or Linear Parameter Varying (LPV) design methodologies [15]. The basic limitation of these approaches is that stability is only guaranteed in a neighborhood of the selected operating points. Moreover, performance can suffer significantly when the vehicle executes maneuvers that emphasize its nonlinearity and cross-couplings.

Nonlinear Lyapunov-based designs can overcome some of the limitations mentioned above. Several examples of

nonlinear trajectory tracking controllers for marine underactuated vehicles have been reported in the literature [4, 5, 12, 14, 18, 19]. Godhavn [12] proposed a backstepping-based continuous time-invariant state-feedback control law for an underactuated surface vessel. The control law provides exponential position tracking as long as saturation of the inputs is avoided and the vehicle surge velocity is nonzero. However, Godhavn's approach requires the ship to move along straight lines or arcs of circles to guarantee stable zero dynamics for the nonlinear system. Pettersen and Nijmeijer [18] consider the kinematics of a surface vehicle and design a time-varying control law for the surge and yaw inputs. Under this controller, the errors in position and orientation with respect to a reference trajectory of constant curvature is practically globally exponentially stabilized to zero. The control law in [18] does not require nonzero reference linear velocity. See also [19], where the same authors present experimental results for a model ship of a Lyapunov-based tracking controller. In [5], a global practical tracking and regulation controller was developed by manipulating a reference model generator and the dynamic model of the vehicle into a suitable form that allows a Lyapunov-based design. Recently, by Lyapunov's direct method and passivity approach, two constructive tracking solutions were proposed in [14] for an underactuated surface ship.

Typically, tracking problems for autonomous vehicles are solved by designing control laws that make the vehicles track pre-specified feasible "state-space" trajectories, *i.e.*, trajectories that specify the time evolution of the linear and angular positions and velocities and that are consistent with the vehicles' dynamics (*e.g.* [5, 11, 14, 18, 19]). This approach suffers from the drawback that the vehicles' dynamics usually exhibit complex nonlinear terms with significant uncertainty, making the task of computing a feasible trajectory hard. Fortunately, in practical applications one often only needs to track the desired position, making it possible to bypass the computation of feasible state-space trajectories.

Motivated by the above considerations, in [3] Aguiar and Hespanha proposed a solution to the position tracking problem for a fairly general class of underactuated autonomous vehicles that is applicable to motion in either two or three-dimensional spaces. The control algorithm proposed builds on iterative Lyapunov-based techniques and it was shown to yield global stability and exponential convergence of the position tracking error to a neighborhood of the origin that can be made arbitrarily small. Furthermore, the desired trajectory does not need to be a specially chosen. In fact, it can be any sufficiently smooth bounded curve parameterized by time.

Despite the variety of approaches that have been proposed to solve the trajectory tracking control problem for underactuated autonomous vehicles, with exception of wheeled mobile robots, there has been relatively few experimental results reported. Experimental results highlight the value and limitations of the control algorithms and trigger the development of new theoretical concepts. In this paper we present experimental results for position tracking control of

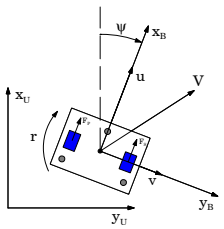


Fig. 2. A schematic of the hovercraft vehicle. Body-fixed $\{B\}$ and earth-fixed $\{U\}$ coordinate frames.

an underactuated hovercraft with three degrees of freedom and two control inputs. The hovercraft is equipped with two high-powered ducted fans that provides the thrust to move the vehicle forward and to make it turn. Contrary to most wheeled mobile robots, this vehicle can move freely sideways even though this degree of freedom is not actuated. Compared to surface ships, the hovercraft has a much smaller damping matrix norm. We build a control algorithm for the MVWT hovercraft based on the design methodology proposed in [3]. In addition, we extend the results in [3] by exploiting the specific properties of the damping matrix for the MVWT. We also design a reference model system which is responsible for generating the desired trajectory and its derivatives for the tracking controller.

## II. The Hovercraft Model and Control Problem Formulation

This section describes the kinematic and dynamic equations for the hovercraft shown in Fig. 1 and formulates the corresponding problem of position trajectory tracking.

### A. Vehicle Modeling

Following standard practice, the general kinematic and dynamic equations of motion of the vehicle can be developed using a global coordinate frame $\{U\}$ and a body-fixed coordinate frame $\{B\}$ that are depicted in Fig. 2. The kinematic equations of motion for the vehicle can be written as

$$\dot{x} = u\cos\psi - v\sin\psi, \tag{1a}$$

$$\dot{y} = u\sin\psi + v\cos\psi, \tag{1b}$$

$$\dot{\psi} = r, \tag{1c}$$

where $u$ (surge speed) and $v$ (sway speed) are the body fixed frame components of the vehicle's velocity, $x$ and $y$ are the Cartesian coordinates of its center of mass, $\psi$ defines the vehicle's orientation, and $r$ its angular speed.

Assuming that the friction forces and moment can be modelled by viscous friction, the dynamic equations of motion are

$$m\dot{u} - mvr + d_\nu u = F_s + F_p, \tag{2a}$$

$$m\dot{v} + mur + d_\nu v = 0, \tag{2b}$$

$$J\dot{r} + d_r r = l(F_s - F_p), \tag{2c}$$

where $m$ is the vehicle's mass, $J$ its rotational inertia, and $d_\nu$ and $d_r$ the coefficients of viscous and rotational friction, respectively. The starboard and portboard fan forces are denoted $F_s$ and $F_p$, respectively, and $l$ denotes the moment arm of the forces with respect to the center of geometry and

mass of the vehicle, which are assumed to coincide. The control inputs $u_1 := F_s + F_p$, and $u_2 := l(F_s - F_p)$ are the pushing force along the vehicle axis $x_B$ and the steering torque about its vertical axis $z_B$, respectively. The hovercraft is underactuated as we do not have an available control in sway. Equations (1) and (2) can be written compactly as

$$\dot{p} = R(\psi)\nu, \tag{3a}$$
$$\dot{\psi} = r, \tag{3b}$$
$$M\dot{\nu} = -S(r)M\nu - D_\nu\nu + gu_1, \tag{3c}$$
$$J\dot{r} = -d_r r + u_2, \tag{3d}$$

where $p = (x, y)'$, $\nu = (u, v)'$, $R(\psi) = \begin{pmatrix} \cos\psi & -\sin\psi \\ \sin\psi & \cos\psi \end{pmatrix}$, $S(r) = \begin{pmatrix} 0 & -r \\ r & 0 \end{pmatrix}$, $M = \mathrm{diag}\{m, m\}$, $D_\nu = \mathrm{diag}\{d_\nu, d_\nu\}$, and $g = (1, 0)'$. Notice that $D_\nu > 0$, which will be exploited in the control design at the backstepping phase.

### B. Problem Formulation

Let $p_d : [0, \infty) \to \mathbb{R}^2$ be a given sufficiently smooth time-varying desired trajectory with its derivatives (with respect to time) bounded. The problem under investigation can be formulated as follows:

*Consider the underactuated vehicle represented by equations* (1)-(2)*. Design a controller such that all the closed-loop signals are globally bounded and the tracking error $\|p - p_d\|$ converges exponentially fast to a neighborhood of the origin that can be made arbitrarily small.*

## III. The Control Law

This section presents a Lyapunov-based control law for the underactuated hovercraft that solves the position tracking problem of Section II-B.

### A. Controller Design

The trajectory controller design follows the general methodology outlined in [3].

*Step 1. Coordinate transformation:* Consider the global diffeomorphic coordinate transformation

$$e := R(\psi)'(p - p_d),$$

which expresses the tracking error $p - p_d$ in the body-fixed frame. The dynamic equation of the tracking error $e$ is given by $\dot{e} = -S(r)e + \nu - R(\psi)'\dot{p}_d$.

*Step 2. Convergence of $e$:* We start by defining the control-Lyapunov function

$$V_1 := \frac{1}{2}e'e$$

and computing its time derivative to obtain $\dot{V}_1 = e'[\nu - R(\psi)'\dot{p}_d]$. We can then regard $\nu$ as a virtual control that we would like to use to make $\dot{V}_1$ negative. This could be achieved, *e.g.*, if one could set $\nu$ equal to $R(\psi)'\dot{p}_d - k_e M^{-1}e$, for some positive constant $k_e$. To achieve this we introduce the error variable

$$z_1 := \nu - R(\psi)'\dot{p}_d + \frac{k_e}{m}\,e,$$

and re-write $\dot{V}_1 = -\frac{k_e}{m}\,\|e\|^2 + e'z_1$.

*Step 3. Backstepping for $z_1$:* After straightforward algebraic manipulations, we conclude that the dynamic equation of the error $z_1$ can be written as

$$m\dot{z}_1 = -mS(r)z_1 + gu_1 + h(e, \psi, z_1, \dot{p}_d, \ddot{p}_d) - D_\nu z_1,$$

where $h := -D_\nu R(\psi)'\dot{p}_d + \frac{k_e}{m}D_\nu\, e - mR(\psi)'\ddot{p}_d + k_e z_1 - \frac{k_e^2}{m}\,e$. It turns out that it will not always be possible to drive $z_1$ to zero. Instead, we will drive $z_1$ to a small constant $\delta$. To achieve this we define $\varphi := z_1 - \delta$ as a new error variable that we will drive to zero and consider the augmented control-Lyapunov function

$$V_2 := \frac{1}{2}e'e + \frac{1}{2}m^2\varphi'\varphi = V_1 + \frac{1}{2}m^2\varphi'\varphi.$$

The time derivative of $V_2$ can be written as

$$\dot{V}_2 = -\frac{k_e}{m}\,\|e\|^2 + e'\delta + \varphi'\big(mB(\delta)\mu + mh - mD_\nu\delta + e\big) - m\varphi' D_\nu\varphi,$$

where $B(\delta) := \begin{pmatrix} 1 & m\delta_2 \\ 0 & -m\delta_1 \end{pmatrix}$ and $\mu := (u_1, r)'$. One can now regard $\mu$ as a virtual control (actually its first component is already a "real" control) that one would like to use to make $\dot{V}_2$ negative. This could be achieved, *e.g.*, if one could set $\mu$ equal to

$$\alpha := -B^{-1}(\delta)\big(h(e, \psi, z_1, \dot{p}_d, \ddot{p}_d) - D_\nu\delta + \frac{1}{m}\,e + \frac{1}{m}K_\varphi\varphi\big),$$

where $K_\varphi \in \mathbb{R}^{2\times 2}$ is a symmetric positive definite matrix. To achieve this we set $u_1$ equal to the first entry of $\alpha$, *i.e.*,

$$u_1 = \begin{bmatrix} 1 & 0 \end{bmatrix}\alpha, \tag{4}$$

introduce the error variable $z_2 := r - \begin{bmatrix} 0 & 1 \end{bmatrix}\alpha$, and re-write $\dot{V}_2$, with $u_1$ given by (4), as $\dot{V}_2 = -\frac{k_e}{m}\,\|e\|^2 + e'\delta - \varphi' K_\varphi\varphi - m\varphi' D_\nu\varphi + m\varphi' B_b(\delta)z_2$ where $B_b(\delta) \in \mathbb{R}^{2\times 1}$ denotes the second column of $B(\delta)$.

*Step 4. Backstepping for $z_2$:* Consider now a third control-Lyapunov function given by

$$V_3 := \frac{1}{2}e'e + \frac{1}{2}m^2\varphi'\varphi + \frac{1}{2}Jz_2^2 = V_2 + \frac{1}{2}Jz_2^2.$$

Computing its time derivative we obtain $\dot{V}_3 = -\frac{k_e}{m}\,\|e\|^2 + e'\delta - \varphi' K_\varphi\varphi - m\varphi' D_\nu\varphi + z_2\big(mB_b'(\delta)\varphi - d_r\begin{bmatrix} 0 & 1 \end{bmatrix}\alpha + u_2 - \begin{bmatrix} 0 & J \end{bmatrix}\dot{\alpha}\big) - d_r z_2^2$. For simplicity we did not expand the derivative of $\alpha$. If we then choose

$$u_2 = -mB_b'(\delta)\varphi + d_r\begin{bmatrix} 0 & 1 \end{bmatrix}\alpha + \begin{bmatrix} 0 & J \end{bmatrix}\dot{\alpha} - k_{z_2}z_2, \tag{5}$$

the time derivative of $V_3$ becomes $\dot{V}_3 = -\frac{k_e}{m}\,\|e\|^2 + e'\delta - \varphi' K_\varphi\varphi - m\varphi' D_\nu\varphi - k_{z_2}z_2^2 - d_r z_2^2$. Note that although $\dot{V}_3$ is not necessarily always negative, this will be sufficient to achieve practical stability.

Following the reasoning in the proof of [3, Theorem 1], the following can be proved:

*Theorem 1:* Given a three-times continuously differentiable time-varying desired trajectory $p_d : [0, \infty) \to \mathbb{R}^2$ with its first three derivatives bounded, consider the closed-loop system $\Sigma$ consisting of the underactuated vehicle model (1)-(2) and the feedback controller (4), (5).

i) For any initial condition the solution to $\Sigma$ exists globally, all closed-loop signals are bounded, and the tracking error $\|p(t) - p_d(t)\|$ satisfies

$$\|p(t) - p_d(t)\| \leq e^{-\lambda t} c_0 + \epsilon, \tag{6}$$

where $\lambda, c_0, \epsilon$ are positive constants. From these, only $c_0$ depends on initial conditions.

ii) By appropriate choice of the controller parameters $k_e, K_\varphi, k_{z_2}$, any desired values for $\epsilon$ and $\lambda$ in (6) can be obtained.

*Remark 1:* Notice that we have not imposed any constraints on the desired trajectory (besides of being sufficiently smooth and its derivative being bounded). Moreover, we also do not require the linear velocity of the vehicle to be always nonzero. Consequently, $p_d(t)$ can be any arbitrary trajectory and in particular can be constant for all $t \geq t_0$. In that case, the controller solves the position regulation problem.

### B. Reference Model

This section describes a reference model system that can be used to generate the desired trajectory $p_d$ and its derivatives for the tracking controller. We recall that $p_d$ must be sufficiently smooth and its derivatives must be bounded. The reference model is needed, *e.g.*, when we want the hovercraft to track a target vehicle. The target vehicle will be viewed as a "black box" (*i.e.*, we do not know its dynamical model) and we assume that only its position can be measured.

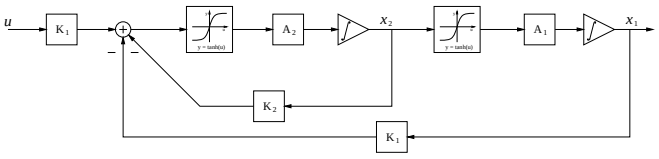


Fig. 3. Block diagram of the pre-filter.

The reference model consists of a cascade of the two second-order nonlinear filters represented in Fig. 3. The input of the first pre-filter is the position of the target vehicle, and the output of the second pre-filter corresponds to the desired position $p_d$ (the input of the controller). The state-space representation of each filter can be written as

$$\dot{x}_1 = a_1 \tanh(x_2) \tag{7a}$$

$$\dot{x}_2 = a_2 \tanh(k_1 u - k_1 x_1 - k_2 x_2), \tag{7b}$$

where it is assumed that $k_1, k_2, a_1$, and $a_2$ are scalar positive constants such that $k_2 a_2 > k_1 a_1$. By linearization, it is straightforward to show that the pre-filter is locally input-to-state stable. Invoking LaSalle's Principle and using the Lyapunov function given by

$$V = \frac{1}{2} e' \begin{bmatrix} \frac{k_1^2}{a_2 k_2} & \frac{k_1}{2 a_2} \\ \frac{k_1}{2 a_2} & \frac{k_2}{a_2} \end{bmatrix} e + \frac{k_1 a_1}{k_2 {a_2}^2} \int_0^{e_2} \tanh(y)\, dy,$$

where $e = (e_1, e_2) := (x_1 - u, x_2)$, it can be proved that for constant input commands ($\dot{u} = 0$), the equilibrium point $x_1 = u$, $x_2 = 0$ of (7) is globally asymptotically stable.

## IV. Experimental Results

The controller in Section III-A and the reference model in Section III-B were validated individually and in tandem using Caltech's MVWT [1]. This section summarizes the results achieved.

### A. Experimental Setup

The Caltech MVWT is an experimental platform for implementation of single- and multiple-vehicle control designs. The MVWT vehicle glides on ball casters on a smooth floor and is propelled by two high-power ducted fans that are fixed to the vehicle. The dynamics of the vehicles are underactuated and input constrained, and exhibit fully second-order dynamic behavior, making it a challenging platform for the investigation of real-time control strategies. The hardware and software environments are carefully designed to minimize the development and implementation times for controller designs. While the results here are described for a single vehicle, the MVWT is especially suited for the development of decentralized and cooperative controller designs.

Each MVWT vehicle consists of a stripped-down laptop (sans screen) mounted in a Plexiglas frame on three low-friction, omni-directional casters. Two high-performance ducted fans are attached to the vehicle, each capable of producing up to 4.5 N of continuous thrust. Fig. 1 depicts the vehicle complete with two NiMH battery packs and a fan interface board. Each vehicle is uniquely identified by markings on a "hat" placed on top of it. These markings are used by the "Lab Positioning System" (LPS) to determine the vehicle's position, orientation, and identity.

Communication between the LPS, the command and control computers and the vehicles is handled by the laptops via 802.11b wireless cards over a local area network. Controller execution programs run on the laptop for autonomous vehicle operation. An electronics interface board connects the laptop (via the USB port) to the two onboard fans, allowing the speed of the motors to be software controlled. Data from optional vehicle sensors — which may include proximity sensors and/or a gyroscope — can be received over the same USB port connection. The reader is referred to [7, 8] for the details of this configuration.

The latest vehicle design measures 25.4 cm deep, 35.6 cm wide and 18.1 cm high. With the casters, laptop, fans, batteries and interface board, the vehicle's mass is approximately 5.15 kg. The other model parameters of the MVWT vehicle (see equation (2)) are $J = 0.047\, kg\, m^2$, $l = 0.123\, m$, $d_\nu = 4.5\, kg/s$, and $d_r = 0.41\, kg\, m/s$.

The control algorithms are implemented in a C++ software environment called RHexLib [2, 16] on the QNX real-time operating system [22]. RHexLib is a *module-based* controller design environment in which each module is given a fixed execution rate, and a module manager performs a static scheduling of the set of modules. The core MVWT modules are `VisionModule`, which processes broadcasts from the LPS; `Controller`, which executes the local control; and `DeviceWriter` which sends the signals to command the fan forces. Each of these modules operates at a sampling

period of $0.016s$ to match the overhead camera frequency of 60 Hz.

The controller described in Section III-A was implemented in two different scenarios. Since the controller takes as inputs the $x$ and $y$ desired position signals and their first three derivatives, it is sufficient to specify these as parameterized functions of time. In Section IV-B we describe an implementation of this option for a specified circular trajectory.

In the absence of a continuously parameterized path description — *e.g.*, when we only has available a sampled-data reference input — we have the options of either generating a parameterized reference signal and its derivatives based on the sampled data, or filtering the sampled data directly. We explore the second option in Section IV-C, by combining the reference model filter described in Section III-B with the controller proposed in Section III-A.

### *B. Following a Prescribed Trajectory*

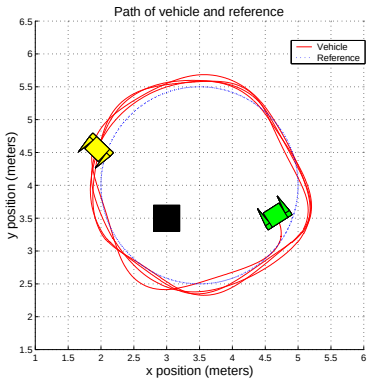


Fig. 4. Vehicle path resulting corresponding to a circular reference trajectory with a constant radius and angular velocity.

The controller of Section III-A was fed with a circular reference trajectory parameterized by time as follows:

$$x_r = x_c + A\cos(\omega_r t + \tau), \tag{8a}$$
$$y_r = y_c + A\sin(\omega_r t + \tau). \tag{8b}$$

The inputs to the controller are the position and orientation of the vehicle, its derivatives in the body-fixed coordinate system, and the reference trajectory along with its first three derivatives. The result of an example run with this controller is shown in Fig. 4. For this data set, the reference parameters are $(x_c, y_c) = (3.5, 4.0)m$, $A = 1.5m$, $\omega_r = 0.3rad/s$ and $\tau = 5.1s$. The controller parameters were $k_e = 4.0$, $K_\phi = \text{diag}(1.5, 1.5)$ and $k_{z_2} = 0.6$.

Data from an onboard gyroscope were not used in the circular reference experiment. The angular velocity signal was computed by finite difference and as a result proved to be particularly noisy. In order to provide a better angular velocity measurements, we implemented a fourth order Butterworth filter with cutoff frequency $f_c = 1.5$ Hz and sample frequency $f_s = 60$ Hz. This reduced significantly the noise content in the computed force output; this noise also tends to be attenuated by the dynamics of the fan assembly.

The reference and actual trajectory followed are shown in Fig. 4, along with the position and orientation of the vehicle at two points on its path. Stability and reasonable performance are achieved in the face of a variety of uncertainties. It is important to emphasize that the model in (1)-(2) assumes perfect actuation and sensing, but in practice the sensing from the LPS is delayed and somewhat noisy, particularly the derivatives which are estimated based on sampled data from the LPS. In addition, for each fan, the maps from the (integer) signal input to the force in Newtons produced by the fan are quantized and may suffer irregularities. Further, the linear model of friction is approximate at best. These modeling considerations are described in more detail in [7].

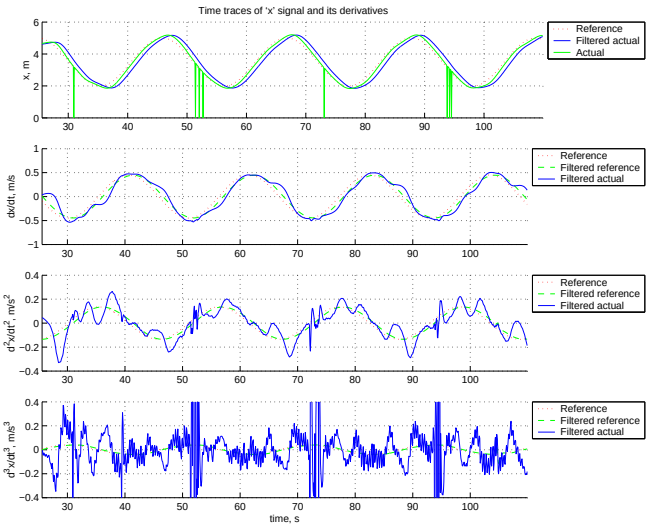


Fig. 5. Time traces of $x$ position and its first three derivatives for the trajectories in Fig. 4. The reference signals are given by dotted lines and the actual signal by the dash-dotted line in the first plot. The filter outputs, given the actual data as input, are shown by solid lines.

### *C. Following a Target Vehicle*

Tests were also performed for a reference input obtained from sampled values of the coordinates $x$ and $y$ obtained from a target vehicle. In this case, the nonlinear filter of Section III-B was used. The parameters in the experiment were $(k_1,\ k_2) = (6.45,\ 3.85)$ and $(a_1,\ a_2) = (1.50, 2.61)$. The filter generated smooth versions of $x$ and $y$ signals and their first three derivatives.

The data set in Fig. 5 shows the performance of the filter when applied to the trajectories in Fig. 4. The figure shows $x$ and its derivatives. The actual $x$ data is shown in the first plot as a dashed line. This value drops to zero a few times which correspond to periods during which the vision system failed to identify the vehicle's location. In practice, at these times the vision module performs a zero-order hold on the previous reliable value. The zeros are included in the signal here to highlight the robustness of the filter. Note that the filtered signal is virtually unaffected by the erratic perturbations at around 52s, 73s and 94s, up to the first derivative. The second derivative is slightly affected and it is only in the third derivative that these perturbations have a significant effect.

Having verified the acceptable performance of the nonlinear filter, it was combined with the nonlinear controller to provide a tracking control system that only takes as input sampled positions of a target vehicle. Experimental data for this scenario is shown in Fig. 6. The same parameters for the controller and filter were used, but an onboard gyroscope replaced the LPS in providing local angular rate information. The target vehicle was controlled manually along the path indicated by the dotted line in Fig. 6(a). The resultant path of the vehicle running our controller and filter is shown solid along with the starting and ending positions of the vehicle.

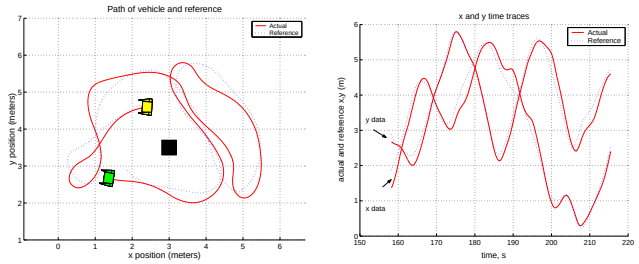


(a) Trajectory of vehicle and reference trajectory.

(b) Time traces for $x$ and $y$ reference and actual signals.

Fig. 6. Path of vehicle and target using the nonlinear pre-filter to provide a reference for the nonlinear controller.

The time traces for the vehicle and target $x$ and $y$ signals are shown in Fig. 6(b) for the same experimental run. Target tracking and following is achieved. The adequacy of this level of performance will depend on the situation and application. It should be noted that while global convergence is proven for the model in the absence of input constraints, the experimental vehicles here have input magnitude constraints as well as input sign constraint (the fans are unidirectional). The target in this particular run remained generally in front of the vehicle, for more arbitrary target tracking additional considerations are necessary to take into account the input constraints.

## V. Summary and Future Work

We considered the position tracking control problem of an underactuated hovercraft vehicle. A nonlinear Lyapunov-based control algorithm was described and it was shown to yield global stability and exponential convergence of the position tracking error to a neighborhood of the origin that can be made arbitrarily small. The desired trajectory does not need to be specially chosen and in fact can be any sufficiently smooth bounded curve parameterized by time. To validate the results presented, we describe two types of experiments: the hovercraft following a circular desired trajectory and following a target vehicle. The experiments showed stability and reasonable performance in the spite of large modelling errors. Future research will address the problem of output measurement and state estimation. Another open problem that warrants further research is the control of underactuated vehicles with input constraints.

## VI. Acknowledgments

This material is based upon work supported by the National Science Foundation under Grant No. ECS-0093762. The work of António Aguiar was supported by a Post-Doc Fellowship PRAXIS XXI from the Portuguese Foundation of Science and Technology.

## References

[1] Caltech multiple vehicle wireless testbed website. URL: http://www.cds.caltech.edu/~mvwt/.

[2] RHexLib. URL: http://sourceforge.net/projects/rhex/.

[3] A. P. Aguiar and J. P. Hespanha. Position tracking of underactuated vehicles. In *Proc. of the 2003 Amer. Contr. Conf.*, Denver, CO, USA, June 2003.

[4] F. Alonge, F. D'Ippolito, and F.M. Raimondi. Trajectory tracking of underactuated underwater vehicles. In *Proc. 40th IEEE Conf. on Decision and Contr.*, Orlando, Florida, USA, December 2001.

[5] A. Behal, D.M. Dawson, W.E. Dixon, and Y Fang. Tracking and regulation control of an underactuated surface vessel with nonintegrable dynamics. *IEEE Trans. on Automat. Contr.*, 47(3):495–500, March 2002.

[6] Francesco Bullo, Naomi Ehrich Leonard, and Andrew D. Lewis. Controllability and motion algorithms for underactuated lagrangian systems on lie groups. *IEEE Trans. on Automat. Contr.*, 45(8):1437–1454, 2000.

[7] T. Chung, L. Cremean, W. B. Dunbar, Z. Jin, E. Klavins, D. Moore, A. Tiwari, D. van Gogh, and S. Waydo. A platform for cooperative and coordinated control of multiple vehicles: The Caltech multi-vehicle wireless testbed. In *Proc. of the 3rd Conf. on Cooperative Contr. and Optimization*, 2002.

[8] Lars Cremean, William B. Dunbar, David van Gogh, Jason Hickey, Eric Klavins, Jason Meltzer, and Richard M. Murray. The Caltech multi-vehicle wireless testbed. In *Proc. of the 41st Conf. on Decision and Contr.*, pages 86–88, 2002.

[9] I. Fantoni, R. Lozano, F. Mazenc, and K. Y. Pettersen. Stabilization of a nonlinear underactuated hovercraft. *Int. J. of Robust and Nonlinear Contr.*, 10:645–654, 2000.

[10] T. I. Fossen. *Guidance and Control of Ocean Vehicles*. John Wiley & Sons, England, 1994.

[11] E. Frazzoli, M.A. Dahleh, and E. Feron. Trajectory tracking control design for autonomous helicopters using a backstepping algorithm. In *Proc. of the 2000 Amer. Contr. Conf.*, Chicago, IL, USA, June 2000.

[12] J. M. Godhavn. Nonlinear tracking of underactuated surface vessels. In *Proc. of the 35th Conf. on Decision and Contr.*, pages 975–980, Kobe, Japan, December 1996.

[13] A. Isidori. *Nonlinear Control Systems*. Springer-Verlag, London, UK, $3^{rd}$ edition, 1989.

[14] Z. P. Jiang. Global tracking control of underactuated ships by Lyapunov's direct method. *Automatica*, 38(2):301–309, 2002.

[15] I. Kaminer, A. Pascoal, E. Hallberg, and C. Silvestre. Trajectory tracking controllers for autonomous vehicles: An integrated approach to guidance and control. *J. of Guidance, Control, and Dynamics*, 21(1):29–38, 1998.

[16] E. Klavins and U. Saranli. Object orient state machines. *Embedded Systems Programming Magazine*, 2002. In Press.

[17] H. Nijmeijer and A. J. van der Schaft. *Nonlinear Dynamical Control Systems*. Springer-Verlag, New York, USA, 1990.

[18] K. Y. Pettersen and H. Nijmeijer. Global practical stabilization and tracking for an underactuated ship - a combined averaging and backstepping approach. In *Proc. IFAC Conf. on Systems Structure and Contr.*, pages 59–64, Nantes, France, July 1998.

[19] K. Y. Pettersen and H. Nijmeijer. Underactuated ship tracking control: theory and experiments. *Int. J. of Control*, 74(14):1435–1446, 2001.

[20] M. Reyhanoglu, A. van der Schaft, N. H. McClamroch, and I. Kolmanovsky. Dynamics and control of a class of underactuated mechanical systems. *IEEE Trans. on Automat. Contr.*, 44(9):1663–1671, 1999.

[21] Shankar Sastry. *Nonlinear Systems: Analysis, Stability, and Control*. Interdisciplinary Applied Mathematics: Systems and Control. Springer, New York, 1999.

[22] QNX Realtime Systems. The QNX real time operating system. URL: http://www.qnx.com/.

[23] John Ting-Yung Wen. Control of nonholonomic systems. In William S. Levine, editor, *The Control Handbook*, pages 1359–1368, Florida, USA, 1996. CRC Press & IEEE Press.